

This is a postprint version of the following published document:

Villoslada, L., Rivera, C., Escudero, N., Martín, F., Blanco, D. & Moreno, L. (2019). Hand Exo-Muscular System for Assisting Astronauts During Extravehicular Activities. *Soft Robotics*, 6(1), 21–37.

DOI: [10.1089/soro.2018.0020](https://doi.org/10.1089/soro.2018.0020)

© 2019, Mary Ann Liebert, Inc., publishers.

# Hand Exo-Muscular System for Assisting Astronauts During Extravehicular Activities

Álvaro Villoslada,<sup>1</sup> Cayetano Rivera,<sup>2</sup> Naiara Escudero,<sup>2</sup> Fernando Martín,<sup>1</sup> Dolores Blanco,<sup>1</sup> and Luis Moreno<sup>1</sup>

## Abstract

Human exploration of the Solar System is one of the most challenging objectives included in the space programs of the most important space agencies in the world. Since the Apollo program, and especially with the construction and operation of the International Space Station, extravehicular activities (EVA) have become an important part of space exploration. This article presents a soft hand exoskeleton designed to address one of the problems that astronauts face during spacewalks: hand fatigue caused by the pressurized EVA gloves. This device will reduce the stiffness of the spacesuit glove by counteracting the force exerted by the pressurized glove. To this end, the system makes use of a set of six flexible actuators, which use a shape memory alloy (SMA) wire as the actuating element. SMAs have been chosen because some of their features, such as low volume and high force-to-weight ratio, make them a suitable choice taking into account the constraints imposed by the use of the device in a spacesuit. Besides describing the different mechanical and electronic subsystems that compose the exoskeleton, this article presents a preliminary assessment of the device; several tests to characterize its nominal operation have been carried out, as well as position and force control tests to study its controllability and evaluate its suitability as a force assistive device.

**Keywords:** soft robotics, wearable robotics, space robotics, hand exoskeleton, shape memory alloy actuator

## Introduction

SINCE THE BEGINNING of the space race in the mid-50s, space exploration has been a subject of increasing importance for governments and agencies worldwide, because of different scientific, technological and economical reasons. Although in the last two decades manned missions have been progressively replaced by robotic missions thanks to the technological advances in this field, human presence still is of great importance in those tasks where robotics is not yet ready to replace human skills, usually tasks that require dexterous manipulation. During these extravehicular activities (EVA), astronauts wear a full-body protective suit that provides environmental protection, mobility, life support, and communications. The spacesuit is an internally pressurized, semirigid equipment made of multiple layers to protect the user from the vacuum of space, radiation, extreme temperatures, and micrometeoroids.

Despite the advances that have taken place over the last decades in spacesuit technology, factors such as suit-induced

trauma, fatigue, or reduced mobility/dexterity still limit the duration of spacewalks during EVA. These problems especially arise in the case of the hands. A study conducted by NASA with 86 astronauts during 770 sessions showed that the subjects suffered injuries in 45.7% of the sessions, and that 47% of those injuries involved the hands.<sup>1</sup> Other studies found that, when using EVA gloves, the astronaut's grip strength was decreased up to 50% of the force exerted with bare hands.<sup>2,3</sup> The decrease in hand strength when performing different tasks with a pressurized glove reported in Appendino *et al.*<sup>4</sup> is more dramatic, being a 80–90% of the bare hand force.

Hand-related injuries and fatigue are caused by the great stiffness of the spacesuit gloves. Like the rest of the suit, EVA gloves are internally pressurized. The pressure inside the gloves, combined with the multiple layers of which they are composed, increase the stiffness of each of their joints, making the astronaut exert great forces to overcome this rigidity and mobilize the fingers. Some studies have quantified the opposing forces exerted by the EVA glove on the hand,

<sup>1</sup>Department of Systems Engineering and Automation, Carlos III University, Madrid, Spain.

<sup>2</sup>ARQUIMEA Ingeniería S.L.U., Madrid, Spain.

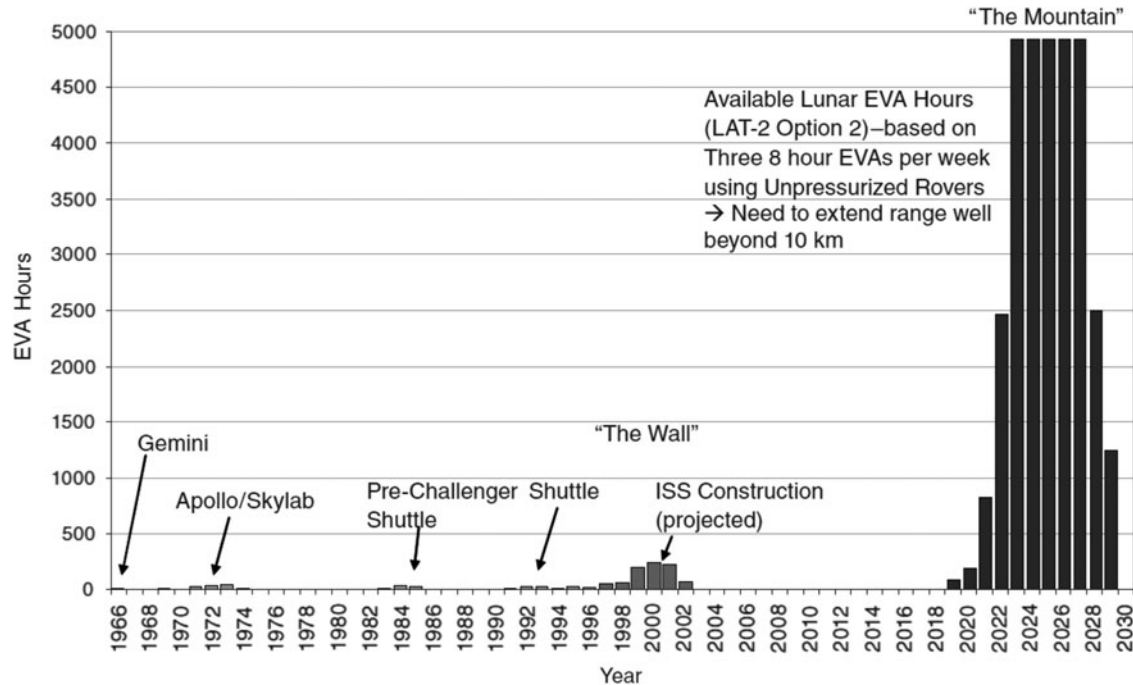


FIG. 1. The mountain of EVA (taken from Walz and Gernhardt<sup>7</sup>). EVA, extravehicular activities.

measured as the integral of all pressures on the whole hand surface, obtaining a mean force of 32 N and peak values of 38 N for power grip.<sup>5,6</sup> The stiffness of EVA gloves leads to problems other than hand fatigue, such as damages in the nails, difficulties to move with dexterity and lack of control of the applied force on the objects. With NASA, as well as other space agencies, planning to dramatically increase the number of EVA hours during future manned missions,<sup>7</sup> a problem known as “the mountain of EVA” (Fig. 1), there is a need for solutions that minimize the negative effects derived from the use of an EVA suit.

With the aim of reducing hand fatigue during EVA missions, several authors have proposed the integration of external actuators, such as gas-filled bladders,<sup>8,9</sup> geared DC motors,<sup>10,11</sup> ultrasonic motors,<sup>12</sup> or pneumatic artificial muscles (PAM),<sup>13</sup> into the EVA glove, to apply an additional torque at the metacarpophalangeal joint of the spacesuit glove and reduce the effort required to move the fingers.

A different approach to overcome the rigidity of EVA gloves is to augment the astronaut's force by means of a hand exoskeleton worn over the glove. Favetto *et al.* devoted several articles to study what features such devices should have, in terms of structure and kinematics, actuators, sensors, and control.<sup>14–16</sup> The most noteworthy examples within this approach are the exoskeletons based on four-bar linkages implemented by Shields *et al.*<sup>17</sup> and Favetto,<sup>18</sup> the flexible fiberglass shell actuated by a single PAM designed by Matheson and Brooker<sup>19</sup> and the low-profile cable-driven finger exoskeleton proposed by Favetto.<sup>18</sup>

Although conventional exoskeletons are an effective solution to overcome the EVA glove stiffness, they have some problems that may prevent their use in a real spacesuit. These devices are usually bulky, which would make the spacesuit gloves even more cumbersome. In addition, NASA limits the working envelope of the glove to specific dimensions, to use

the different tools and interfaces required on EVA missions, so any device attached to the glove can not exceed these dimensions.\* Another problem is the added weight when wearing the exoskeleton, which increases the inertia in the astronaut's limbs. Finally, exoskeletons have to be carefully designed from a kinematic point of view. The kinematic chain of the wearable robot overlaps that of the human body, and, as the latter is very complex and difficult to replicate, usually the differences between the two cause interaction forces, joint misalignment and motion restrictions, which ultimately cause discomfort and difficulties in controlling the device.<sup>20</sup>

However, soft exoskeletons, a new type of exoskeleton that has emerged in recent years from the conjunction of soft robotics and wearable robotics, have some features that make them an appealing option to solve the astronaut's hand fatigue problem. In a soft exoskeleton, the rigid frame of a conventional exoskeleton is replaced by textiles that transmit the forces generated by the actuators to the user's limbs and provide support for the actuators, electronics, and power sources. By getting rid of the rigid frame, a soft exoskeleton is usually lighter and also avoids problems related with joint misalignment that conventional exoskeletons usually have, providing a minimal impediment to the wearer's motions. The downside of this approach is that, in the absence of a rigid structure, the user's skeleton must withstand the external loads as well as the forces generated by the actuators.

Most soft hand exoskeletons in the literature are designed to be used in the rehabilitation field. The mechanical structure of these devices consists of a glove, which serves as the interface that transmits the motion of the actuators to the user's fingers. Using a glove as the supporting element of a hand exoskeleton

\*NASA-STD-3000/T

fulfills the features of flexibility, absence of rigid elements, low volume, and comfort that characterize soft exoskeletons. These devices are mainly actuated either by DC motors<sup>21–25</sup> or by fluidic elastomeric actuators (FEAs).<sup>26–30</sup>

Exoskeletons within the first category are cable-driven devices in which the actuators produce a linear motion and do not transmit torque directly to the biological joints, but rather transmit the generated force remotely by means of cables. The main advantage of this type of actuation system is that the cable transmission allows the actuators to be placed away from the hand, reducing the weight of the hand exoskeleton itself. However, the contribution of the actuators to the total mass of the device remains significant since the weight and volume of DC motors can only be reduced to a certain extent, given the force requirements of wearable devices. Moreover, DC motors are made of rigid materials, which is not consistent with the design philosophy of soft robots.

FEAs, on the other hand, are a relatively new type of actuators designed according to the soft robotics approach. Made of compliant and flexible materials and using a pressurized fluid as their driving force, FEAs are generally designed to produce a bending motion, although they can also be designed to provide linear and twisting motions, or any combination of them. Motion primitives are defined by the stiffness of the material<sup>29</sup> or by using an external fiber matrix whose pattern defines what motions the actuator generates.<sup>31,32</sup> The biggest drawback of these actuators is that they require a pressure source, usually a compressor, to provide the driving force. Ultimately, this means that the whole actuation system requires a rigid, bulky, and heavy element, as is the case with DC motor-based actuation systems, which limits their miniaturization and wearability.

The soft exoskeleton design paradigm has some significant benefits regarding the integration of a wearable robot into a spacesuit. Being flexible, a soft exoskeleton will not make the spacesuit stiffer. Unlike rigid exoskeletons that usually hinder the natural motions of the user's limbs, soft exoskeletons are more compliant from a kinematic point of view, reducing the restrictions to the wearer's movement. Since the stiff nature of spacesuits already obstructs the astronaut's normal range of motion, this feature of soft exoskeletons is an additional advantage regarding their use in EVA activities. Finally, the lower bulkiness of soft exoskeletons with respect to their rigid counterparts implies an easier integration into existing spacesuits.

Being a relatively new field, there are very few examples of the soft robotics approach applied to the design of power-assisted EVA gloves. Freni *et al.* carried out a preliminary study of possible actuation and sensing technologies that could be used in the design of a soft hand exoskeleton intended to be integrated into a spacesuit glove.<sup>33</sup> Electroactive polymers, and more specifically dielectric elastomers, were proposed as the transducer element of a new soft actuator, which was only theoretically studied but not implemented.

NASA along with General Motors designed the RoboGlove, a force augmentation glove based on the actuation system of the Robonaut humanoid robot, to be used in heavy-duty and repetitive assembly tasks, as well as in augmented spacesuit gloves.<sup>34</sup> With a cable-driven actuation system operated by three linear DC actuators located on the forearm of the glove, the device was able to exert a peak grasp force of about 220 N and a continuous grasp force of 67–89 N. Con-

tinuing with this line of work, Rogers *et al.* developed the Space Suit RoboGlove (SSRG) as a result of integrating the RoboGlove technology into a Phase VI EVA glove.<sup>35,36</sup> The SSRG was tested inside a depressurized glove box that simulated the operating pressure of a real spacesuit, revealing that the device was able to provide a grasping force of ~45 N additional to that exerted by the test subjects, and that the average grip strength was higher and more consistent as the subjects became fatigued when compared with the results obtained with the assistive system turned off.

## Objective

This work presents the Hand Exo-Muscular System (HEMS), a soft hand exoskeleton designed to prevent astronauts from exerting all the force needed to mobilize the fingers when wearing an EVA glove, to mitigate hand fatigue and the other hand-related problems that arise during EVA missions. The HEMS, shown in Figure 2, is intended to be embedded into the spacesuit glove, so it should not add any additional volume or stiffness. For this reason, the exoskeleton has been designed following the soft robotics approach.

To establish the amount of assistive force the HEMS should deliver, let's first consider the maximum force exerted by the human fingers at the tip, which according to Sutter *et al.* is 49 N.<sup>37</sup> If, as stated before, the EVA glove reduces the astronaut's grip strength to a 50% of the force exerted with bare hands, this means that a normal force of 24.5 N have to be applied at the fingertips to flex the fingers. According to Hadi *et al.*,<sup>38</sup> the normal force at the fingertips in a tendon-driven robotic glove similar to the HEMS is a 35% of the pulling force applied to the tendon. This means that, for the device to exert all the force necessary to counteract the rigidity of the glove, the actuators must be capable of exerting 70 N of force. This means that, if the device has to provide all the necessary force to counteract the rigidity of the glove, the actuators must be able to provide 70 N of pulling force.

Given this force requirement, and the volume and weight constraints imposed by the integration of the HEMS into an EVA glove, shape memory alloys (SMAs) have been used to design the device actuators because, according to Hirose *et al.*,<sup>39</sup> they have a performance equivalent to that of electric motors and, within the category of lightweight actuators (below 100 g), they have the highest power-to-weight ratio. To avoid using large-diameter wires with a very low actuation bandwidth, the HEMS assistive force will be defined as a 50% of the force required to overcome the opposing force of an EVA glove, that is, 35 N.

A series of characterization tests have been performed to study the behavior of the exoskeleton. Finally, to assess whether it is possible to provide a controlled assistive force with the HEMS, a force controller for the actuation system has been implemented and tested. To control the position of the user's fingers, a position controller has also been developed and tested.

One of the main contributions of this work with respect to previous developments in the field is that, to the best of our knowledge, this is the first controlled SMA-actuated hand exoskeleton. There are very few examples of SMA-actuated hand exoskeletons in the literature<sup>38,40–42</sup> and none of them is able to control the amount of assistive force they provide nor the position of the user's fingers. In those works, the authors only carried out characterization tests or open-loop control tests using simple on-off controllers.



**FIG. 2.** HEMS overview. HEMS, Hand Exo-Muscular System.

This is also the first SMA-actuated hand exoskeleton to apply the soft robotics approach to both the structure of the device and to its actuation system. The wrist orthosis presented in Dittmer *et al.*<sup>40</sup> is a completely rigid device and the mechanical structure of the exoskeleton in Tang *et al.*<sup>41</sup> is based on rigid linkages. While the devices presented in Refs.<sup>38,42</sup> use a glove as the interface to transmit the force and motion of the device to the user's fingers, their actuation systems consist of rigid structures that do not exploit the deformable nature of SMAs.

This work significantly extends our previous research on the design and control of soft SMA actuators and presents the application of the concepts developed in these preceding works in a real device. Building on the flexible SMA actuator design presented in Refs.,<sup>43,44</sup> we have developed a new actuator that integrates position and force sensing and that includes an output mechanism that allows reducing the length of the SMA element by multiplying its displacement. Compared with our previous work, this new actuator is a more polished device that can be potentially deployed on different types of soft wearable robots. We have also extended the application of the bilinear proportional-integral-derivative (BPID) controller presented in Villoslada *et al.*,<sup>45</sup> using it for the first time to the control of the force exerted by an SMA actuator.

## Materials and Methods

### Design

Rather than as an exoskeleton, the presented system can be defined as an exomusculature. Designed according to the soft exoskeleton design paradigm, there is no external rigid structure and the actuation system, consisting of a set of linear actuators connected to the fingers through a series of artificial tendons, somehow mimics the musculotendinous system of the human hand.

The central element of the HEMS is the actuation system, which consists of six flexible SMA linear actuators that assist the user in flexing the fingers. Besides the actuation system, the HEMS is composed of the suit structure, which is the physical layer into which the actuating and sensory systems

are integrated and which transmits the forces generated by the actuators to the user's fingers, and the sensory system, a set of force and position sensors for the actuators. The control hardware uses the information provided by the sensory system to control the actuation system in such a way that the adequate assistive forces are provided. A power supply unit provides the required power to the actuators, sensors, and control electronics.

**Suit structure.** In the case of a conventional exoskeleton, the rigid structure of the device provides the mechanical support and anchoring points for the actuators, sensors, control hardware, batteries, and so on. Although in a soft exoskeleton there is no rigid structure, some kind of support element is required to attach all the hardware to the wearer's body, as well as some kind of mechanical interface to transmit the displacements and forces generated by the actuators to those parts of the body upon which the device acts. In the case of the HEMS, the suit structure is composed of a body harness, a forearm elastic sleeve and a glove, as can be seen in Figure 2.

The glove is the most important element of the suit structure: it is the mechanical interface that transmits the forces generated by the actuators to the user's fingers. The actuators are connected to the glove through a series of inextensible cords attached to the fingertips and routed through the underside of the fingers and the palm of the glove, mimicking the tendon system of a human hand. The function of this artificial tendon system is to transmit the force and linear motion of the actuators to the fingertips of the glove, causing the user's fingers to flex. The index, middle, ring, and little fingers have only one tendon each, whereas the thumb has two tendons: one attached to the tip to perform the flexion movement, and a second one attached to the base of the thumb to perform the abduction movement. This arrangement makes a total of six actuated degrees of freedom. While the flexion of the fingers is active, the extension movement does not need to be actuated, as the opposing force exerted by the internal pressure of the EVA glove causes the hand to tend to be open.

Figure 3a shows the arrangement of the HEMS tendon-based transmission system. Each artificial tendon is routed from the output of an actuator to the base of its corresponding finger through a flexible nylon tube with one end fixed to the actuator and the other end sewed to the palm of the glove. From this point, the tendon is guided over the underside of the finger up to the fingertip of the glove, where it is fixed. Two plastic rings located on the proximal and medial phalanges keep the tendon in place, close to the finger, and transmit the force generated by the actuator to the dorsal side of the phalanges. To fix the tendon to the fingertip, it forms a loop over the dorsal side of the distal phalanx so that, when a tensile force is applied to the tendon, a normal force is applied to this side of the finger, leading to its flexion and reducing the deformation of the glove.

Due to the impossibility of using a real EVA glove, for testing purposes the HEMS external glove is a heavy-duty rubber glove (Fig. 3b). A heavy-duty glove has been chosen because, due to its thickness, it impedes the natural motion of the wearer's fingers in a somehow similar manner than a pressurized EVA glove.

**HEMS actuation system.** The HEMS actuation system is based on the flexible SMA linear actuator presented in Refs.<sup>43,44</sup> An SMA wire is used as the transducer material of the chosen actuator because of its advantageous properties in terms of actuation force, weight, and volume, which allows the design of compact and lightweight, yet powerful, actuators, suitable for wearable robotics and space applications. SMA linear actuators are not exempt of limiting factors, such as their nonlinear behavior, low output displacement with respect to their length, low actuation bandwidth, and low efficiency. As will be detailed below, the mechanical design of the used flexible actuator improves the actuation bandwidth and implements a practical solution to the need of using a very long wire to obtain the required linear displacement to fully flex a finger. The approach used to tackle the nonlinear operation of SMAs, which affects the control of the actuator, is detailed in Actuator Control Section.

An SMA is a metallic alloy that can recover its original "memorized" shape after being deformed when heated above a specific range of temperatures, due to a transition between a martensite phase (low temperature) and an austenite phase (high temperature). An SMA actuator uses an SMA element as the transducer material to convert thermal energy into mechanical work. If an electrical current is applied to the SMA actuator, two transduction processes take place. First, electrical energy is transformed into thermal energy thanks to the Joule effect. This thermal energy triggers

the shape recovery process of the SMA element and the resulting recovery energy is transformed into mechanical work. When used in the form of a wire in tensile deformation, the shape memory effect manifests as a linear deformation: when the wire is heated, its length is shortened, and while it cools below its martensite transformation temperature, it gradually recovers its original length, provided that a bias force is applied. However, SMA wires subjected to an axial stress produce low strains, typically 2–5% of their length (they can reach up to 8–10% at the expense of reducing their service life). This implies that in applications where great linear displacements are needed, which is the case of the HEMS, very long SMA wires have to be used.

To design a high-displacement compact SMA actuator, the common approach is to wrap a long wire around a pulley array.<sup>38</sup> The drawback of this solution is that as the length of the wire increases, more pulleys are needed to keep the actuator compact, increasing the complexity and weight of the actuator and its frictional losses. Moreover, this type of solution is hardly compatible with the design of a flexible actuator that fits the soft robotics design approach. The SMA actuators used in the HEMS actuation system follow a different design approach. Instead of reducing the length of the actuator by folding a long SMA wire, the actuator houses the wire in its entire length, but with a flexible design that allows to bend it while it preserves its ability to transmit force and motion. In this way, the long actuators can produce the necessary displacement to flex the user's fingers and can be bent to adapt to the shape of the structure in which they are installed, which in this case is the HEMS wearer's body. The mechanical design of the presented SMA flexible actuator is based on the Bowden cable transmission system, with an approach similar to the designs described in Refs.<sup>46,47</sup>

The flexible element of the actuator is a multilayer sheath consisting of a polytetrafluoroethylene (PTFE) inner tube to reduce friction losses and a helical stainless steel outer sheath that is rigid enough not to be deformed when the SMA wire contracts, but at the same time it is flexible so the actuator can be bent. One important outcome of this configuration with respect to the actuator performance is that it acts as a heat sink, increasing the actuation frequency by reducing the cooling time of the SMA wire, thanks to the greater surface area of the actuator, which greatly increases heat rejection compared with a bare SMA wire. The multilayer Bowden sheath has another advantageous feature regarding SMA actuation: it reduces the thermal runaway effect in the SMA wire. The accelerated temperature increase of the SMA wire during contraction is absorbed and attenuated by the thermal

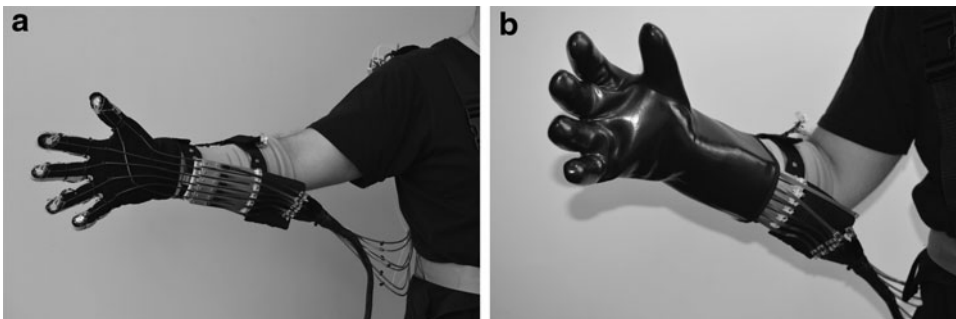


**FIG. 3.** HEMS glove: (a) internal glove with the tendon and actuation systems and (b) external glove.

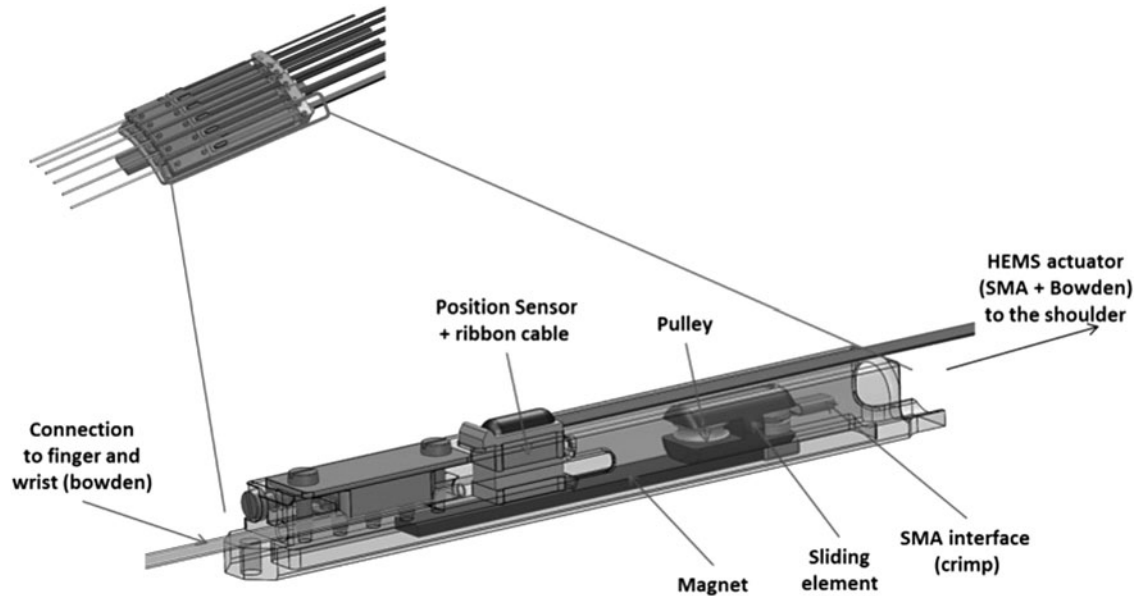


FIG. 4. Elements of the SMA actuation unit. SMA, shape memory alloy.

conduction of both PTFE and steel. This has a beneficial effect on the control of the SMA actuator, as the overshoot that takes place when the wire is commanded to contract is greatly reduced, even eliminated.

The moving ends of the SMA wires are not directly connected to the tendon system that connects them to the HEMS fingers. Each actuator has an additional interface, an actuation unit that includes a displacement multiplier and a linear position sensor, which can be seen in Figure 4. As said before, not to degrade the service life of the actuator, the contraction of the SMA wire is limited to a 3% of its total length. To fully flex the user's index finger with the HEMS, a linear displacement of 5–6 cm is required, which, with the aforementioned contraction limitation, implies the use of a 2-m-long SMA wire. Despite the flexibility of the actuators that would allow routing them along the user's arm and back, this is quite a long actuator. To avoid using such a long wire, a simple pulley interface connects its moving end to its corresponding artificial tendon of the transmission system. This pulley doubles the displacement of the SMA element so that by using a shorter wire, the linear displacement at the output of the actuator is on the desired range. The drawback of this solution is that the pulling force generated at the output of the actuator is reduced to half the force exerted by the SMA wire. Using this displacement multiplier mechanism, the length of the wire used in the actuator has been reduced to 90 cm.

The pulley is installed at one end of a sliding element guided inside the enclosure of the actuation unit. The moving end of the SMA wire is attached to the other end of the sliding element, so that it is displaced by the motion generated by the wire. The artificial tendon that connects the output of the actuator with the finger it actuates runs over the pulley, having one end attached to the fingertip and the other end fixed to the enclosure of the actuation unit, which is an equivalent assembly to a block and tackle mechanism. In this way, when the sliding element of the actuation unit is displaced by the SMA wire, the displacement of the tendon is twice that of the sliding element.

The displacement of the sliding element, and therefore of the SMA wire, is measured by a RoLin linear incremental quadrature encoder<sup>†</sup> fixed to the enclosure of the actuation unit. The sensor measures the displacement of a multipole magnetic strip installed on the sliding element. The actuation unit also provides a fixing point for the multilayer Bowden sheath, as well as a fixing point for the nylon Bowden sheath that routes the artificial tendon from the output of the actuator to the base of its corresponding finger.

To ensure the proper operation of the actuators, the distance between their output and the actuation points (the fingertips of the HEMS internal glove) must be kept constant. If the actuators were fixed to the user's forearm, this condition would not be met if, for example, the user flexed the wrist, in which case the transmission tendons would be slack and the force and displacement generated by the actuators would not be properly transmitted to the fingers.

To avoid the influence of the position of the hand on the operation of the actuators, the six actuation units are installed on a mobile platform which slides over a rail sewed to the forearm elastic sleeve, parallel to the user's forearm. The displacement of the mobile platform is coupled to the angular motion of the wrist on the sagittal plane so that when the wrist is flexed, the platform slides backward, and when the wrist is extended, the platform moves forward, as shown in Figure 5. As detailed in Suit Structure section, six nylon sheaths connect the base of the fingers of the HEMS internal glove to the output of the actuators, as shown in Figure 3a. In addition to guiding the tendons, they also serve to keep the distance between these points constant, regardless of the position of the hand. Also, this set of nylon sheaths is the mechanical interface that transmits the angular motion of the wrist to the moving platform.

The other attachment point of the HEMS actuation system consists of three plastic modules located on the back of the

<sup>†</sup><https://www.rls.si/en/rolin-linear-incremental-magnetic-encoder-system>

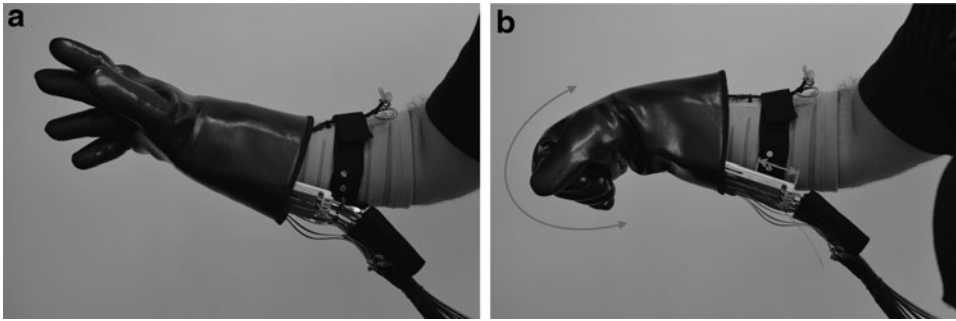


**FIG. 5.** Displacement of the mobile platform: (a) initial position with extended wrist and (b) position after wrist flexion.

user's right shoulder, sewn to the body harness, as shown in Figure 6b. Each shoulder module serves as the fixing point for two SMA actuators, providing a constant mechanical reference point for both the Bowden sheath and the SMA wire that compose each actuator. Also, each shoulder module houses two force sensors, specifically developed for this application by SENSODRIVE,<sup>‡</sup> to measure the stress of the two SMA transducers of the actuators fixed to the module. These sensors can measure forces up to 50 N and their application is twofold: the measured force is used as the feedback signal by the force controller and also as a safety measure to prevent the SMA transducer from reaching values that could harm the user or damage the actuator.

A shoulder module is composed of three elements (Fig. 6a): a coupling interface, which is the part of the module that is sewn to the body harness, and two mechanical interfaces, each of which houses a force sensor and provides the attachment point for the Bowden sheath of one actuator. The SMA wire is fixed to the measuring part of its corresponding force sensor, so that the pulling force exerted by the actuator can be measured. Thanks to the arrangement of the shoulder modules, the HEMS actuation system can be easily attached to and detached from the suit structure, making the donning and doffing of the exoskeleton easier.

The chosen SMA transducer is a Flexinol HT wire, with an austenite start temperature of 90°C, a diameter of 0.5 mm, and a nominal pull force of about 35 N.<sup>48</sup> A wire with these characteristics has been selected because, while wires with a smaller diameter have a greater actuation bandwidth, the force they can exert is not high enough to meet the force requirement defined in the Objective section for this device. A thicker wire capable of providing a greater force could be used, but its cooling time would be too high, which would negatively affect the actuation bandwidth of the device.

The total weight of the HEMS is <1.5 kg and, with the exception of the shoulder modules, has a very low volume, which was one of the design objectives. Each of the HEMS actuators weighs ~150 g, a substantial reduction compared with the 268 g of the SSRG actuators,<sup>35,36</sup> which is the most similar device to the HEMS in terms of its intended use and design philosophy. This is the major advantage of using SMAs over conventional actuation technologies. Thanks to their high force density, it is possible to design actuators with a performance comparable to that of DC motors or pneumatic actuators, but with a fraction of their volume and weight.

The designed actuation system is very similar to cable-driven systems, but with a significant improvement that sets it apart from the latter: while cable-driven devices have the weight of the actuation system concentrated at the location where the actuators are installed, the weight of the flexible SMA actuators is distributed along its entire length, making the whole device more comfortable to wear. One can think of the designed actuator as a cable-driven system in which the transmission element is also the active element, unlike conventional cable-driven systems where the active element, the actuator, the transmission, and the cable, are separate entities.

**Control hardware.** The SMA wire transducers of the HEMS actuation system are heated by means of the Joule effect. Electrical current is supplied by a 16-channel power driver specifically designed to power SMA. Each channel consists of a power MOSFET (STMicroelectronics STP310N10F7) commutation circuit driven by a pulse width-modulated (PWM) signal from the control electronics, powered at 20 V and 4 A, making the maximum input power of each actuator 80 W. PWM commutation has been chosen because, according to Ma and Song,<sup>49</sup> it reduces the actuator energy consumption and makes it more robust to external disturbances.

The low-level controllers of the HEMS actuation system have been implemented in a high-performance, low-cost 32-bit microcontroller unit: the STM32F407VG.<sup>§</sup> The control hardware is in charge of reading and processing the force and position measurements from the corresponding sensors in the actuation system, running the control loops using this information as the feedback signals and generating the PWM control signals to operate the actuator drivers. The control hardware also handles the communication with a host PC over a serial USB connection. Through this data link, the microcontroller receives manual control commands and sends all the relevant information for a real-time monitoring of the system status and performance, information that can be stored for further analysis.

#### *Actuator control*

The HEMS low-level control approach is the four-term BPID controller proposed in Villoslada *et al.*<sup>45</sup> to control the position of SMA actuators. This control strategy has proven to be very effective in controlling this type of actuators despite their nonlinear behavior, and its implementation in embedded systems is simpler than the more complex

<sup>‡</sup><https://www.sensodrive.de/EN>

<sup>§</sup>[www.st.com/en/microcontrollers/stm32f407vg.html](http://www.st.com/en/microcontrollers/stm32f407vg.html)



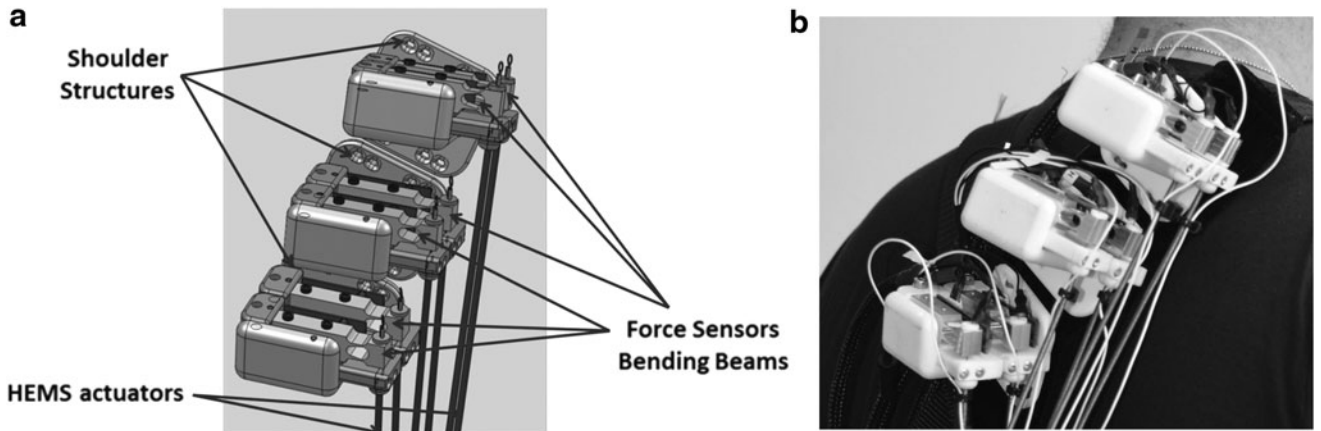


FIG. 6. (a) Elements of a shoulder module and (b) location of the shoulder modules on the suit structure.

strategies that are usually applied to control SMA actuators. For a more in-depth explanation of the theoretical background of the BPID controller, the reader can consult the cited reference.

The proposed BPID control system is essentially a combination of a standard linear PID controller cascaded with a bilinear compensator. The addition of a bilinear compensator can result in a certain linearization of a nonlinear plant, allowing the use of a conventional PID controller. The control output computed by the PID controller is multiplied by the bilinear compensator term proposed by Martineau *et al.*,<sup>50</sup> expressed as:

$$\frac{1 + K_b y_{ref}(k)}{1 + K_b y(k-1)}, \quad (1)$$

where  $K_b$  is the bilinear gain,  $y_{ref}(k)$  is the setpoint at which the PID controller is tuned, and  $y(k-1)$  is the value of the controlled variable in the previous time step.

The developed control scheme has been used to implement a position controller using the HEMS linear position sensors as the source of the feedback signal, as well as to conduct preliminary force control tests using the HEMS force sensors as the feedback devices.

## Results

Several tests have been carried out to characterize the HEMS and to evaluate the performance of the actuator controllers. However, the device has not been tested with human subjects and all experiments have been performed on a test bench that includes a 3D printed human hand dummy. The device has been manually controlled from a host PC.

Only the index finger actuator has been installed on the test bench to perform the different tests. To simulate the stiffness of an EVA glove and to provide the pulling force needed to restore the initial length of the SMA wire during the cooling phase, a bias spring has been used. The spring is connected to the fingertip of the index finger by means of an inextensible cord routed through the dorsal side of the internal glove in an antagonistic configuration relative to the actuator. In these tests, the stiffness of the EVA glove has been simulated with a bias spring instead of with the heavy-duty external glove

shown in Figure 3b because the characteristics of the spring are readily available, whereas those of the heavy-duty glove are unknown, which implies a greater control over the performed experiments.

Since the position sensor measures the displacement of the SMA wire and the force sensor measures its stress, it must be noted that all the measurements presented here refer to the wire and not to the actuator output. As explained in HEMS Actuation System section, the position is doubled while the force is reduced by half at the actuator output, due to the multiplying pulley.

In the first place, the actuation system has been subjected to characterization tests with the purpose of evaluating its performance in terms of nominal and maximum displacement and nominal and maximum force. Also, the influence of the Bowden sheath when varying the geometry of the actuator has been studied. The other set of tests is designed to assess the performance of the actuator position and force controllers.

### Characterization

To ensure a proper operation of the SMA wire during the characterization tests, the actuator has been preloaded with a constant force of 30 N, provided by a hanging mass, and a bias spring pretension force of 20 N, making a total preloading force of 50 N. To characterize the nominal operation of the actuator, the input signals have been different current pulses with a fixed amplitude of 4 A and a variable duration ranging from 1 to 3 s, in 0.2 s increments. As the measured wire resistance is 3.6  $\Omega$ , the input power has been 57.6 W. The most stable behavior has been obtained with a pulse of 1.6 s. From 1 to 1.6 s, there is a 5 mm increment in the actuator output displacement, whereas from 1.6 to 3 s, this difference is only 1 mm. The problem of using longer pulses is that, as more energy is used to drive the actuator, the cooling time can be up to three times longer than when using shorter pulses, as can be seen in Figure 7a. For the 1.6 s pulse, the input energy has been  $57.6\text{W} * 1.6\text{s} = 92.16\text{J}$  per contraction, the maximum displacement has been 29 mm (3.22% strain), and the cooling time has been 4.5 s.

Along with the displacement, the force exerted by the actuator has been measured during the characterization tests, as shown in Figure 7b. For a 1.6 s pulse, the exerted force has a peak value of  $\sim 63\text{N}$ , whereas the SMA wire can produce a

maximum pulling force of 70 N for pulses of 2.2 s or longer. Considering that, because of the pulley of the actuation mechanism, the output force is half this force, the actuator is capable of providing 50% of the force required to move the fingers in an EVA glove as stipulated.

As already discussed in the HEMS Actuation System section, the steel outer sheath of the actuator acts as a heat sink, slightly increasing the convection heat transfer rate and thus reducing the cooling time of the SMA wire. This outcome can be seen in Figure 8a, which shows the variation of the controlled position of a bare SMA wire and of the same wire inside the multilayer sheath. For data in Figure 8a, the cooling time, taking into account that the manufacturer assumes that the wire has cooled when it reaches a deformation of 0.5% of its initial length,<sup>48</sup> has been 4.83 s for the bare SMA wire and 3.33 s for the wire inside the Bowden sheath, which represents a cooling time reduction of more than 30%.

Finally, the effect of the Bowden sheath bending angle on the actuator operation has been analyzed. For this purpose, the bending angle has been increased from 0° to 180° in 10° increments while keeping the bending radius at a constant value of 20 mm. For each angle, the actuator has been driven by the same signal, a current pulse with an amplitude of 4 A and a duration of 2.2 s, and the maximum position and force values

have been measured for each case. The results of this test are shown in Figure 8b, where it can be seen that the relationship between the variation of both measurements is almost linear, which makes sense considering that the variation in the opposing force is due to the displacement of the bias spring.

While the maximum attainable position is reduced by 16.2%, the maximum force decreases by only 4.5%. However, it should be noted that force measurements are biased by the preloading force of 50 N. If this value is subtracted from the maximum force measurements to take into account only the force exerted by the SMA wire to displace the bias spring, the force reduction percentage corresponds to that of the displacement. These results are consistent with the theoretical force transmission efficiency in a Bowden cable transmission given by the Capstan equation<sup>51</sup>:

$$\frac{F_{out}}{F_{in}} \cong e^{-\mu\Theta} \quad (2)$$

where  $\mu$  is the coefficient of sliding friction and  $\Theta$  is the sum of all bending angles along the Bowden sheath. Applying Equation (2) to our case, with a  $\mu_{PTFE} = 0.04$  and a  $\Theta = \pi$  rad, the force transmission efficiency is  $F_{out}/F_{in} \cong 0.88$ , which is very close to the value of 0.84 obtained experimentally.

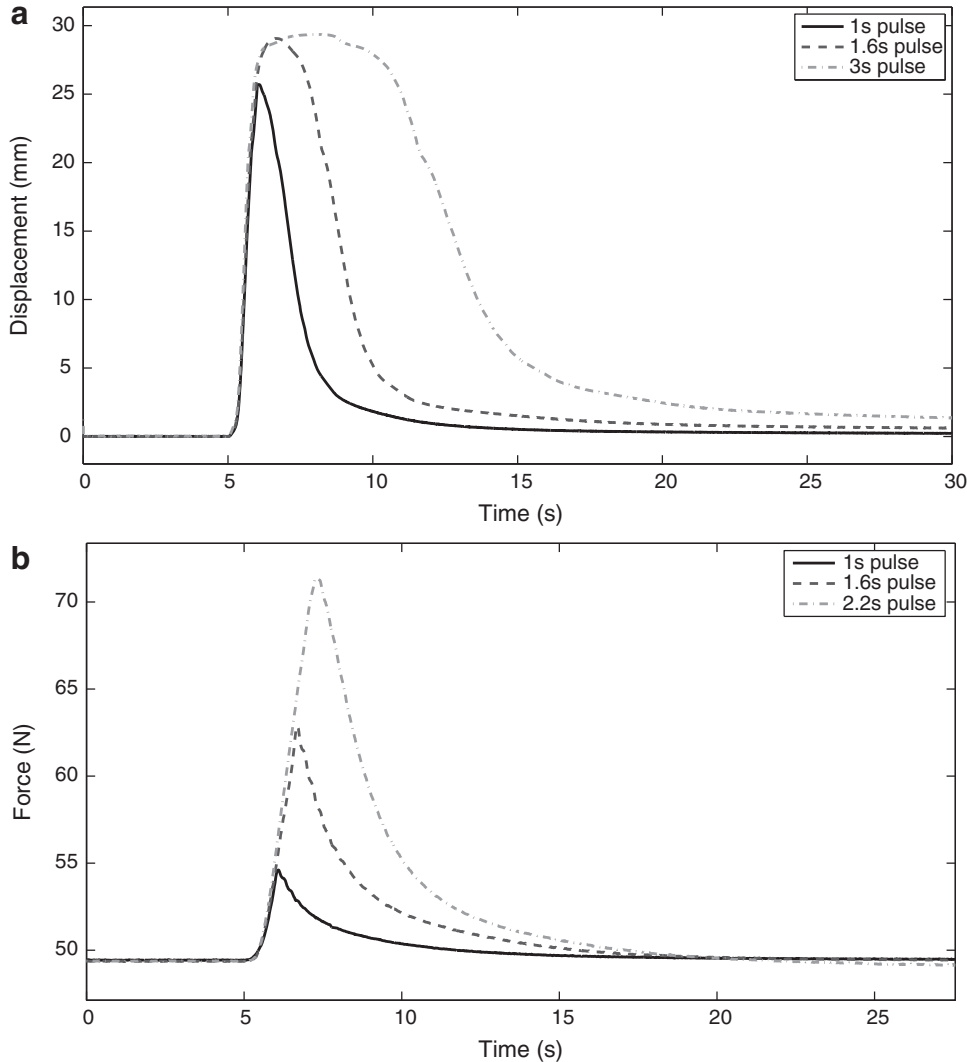


**FIG. 7.** HEMS actuator output depending on input pulse duration: (a) displacement and (b) force.

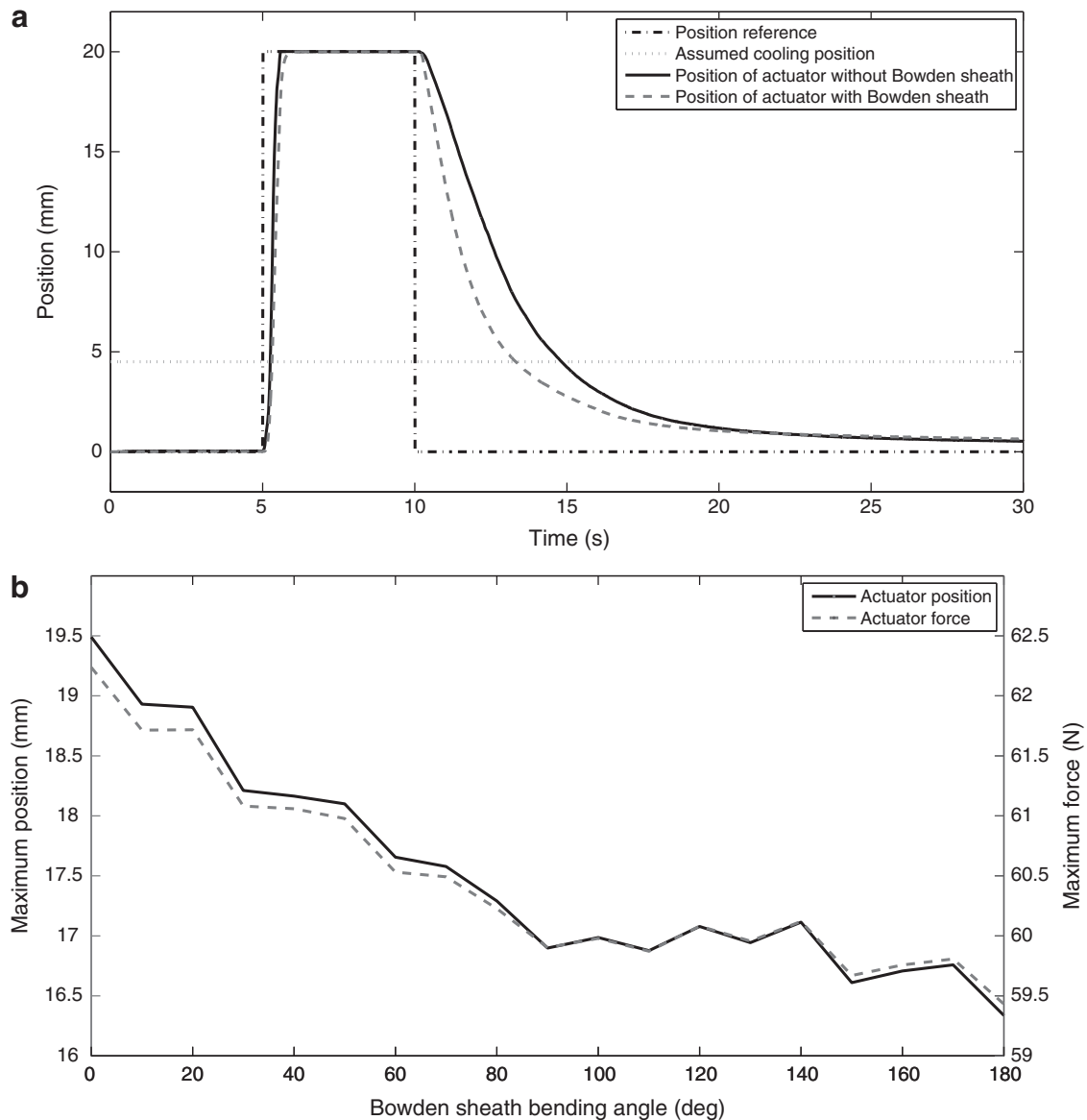


**FIG. 8.** Influence of the Bowden sheath: (a) SMA wire cooling time and (b) actuator performance depending on bending angle.

#### Position control

To evaluate the performance of the BPID control loop in controlling the output position of the HEMS actuator, a set of four different position references with a maximum amplitude of 27 mm have been used. A sinusoidal reference of 0.125 Hz and a ramp reference with a slope of 1 mm/s have been used to study the operation of the controller when following continuously varying references. A step reference and an incremental step reference have also been used to test the stationary behavior of the controlled actuator as well as its performance upon sudden position changes, both large and small.

The preloading force of the actuator has been modified for both the position and the force control tests. The hanging mass has been removed and the bias spring has been pre-tensioned to an opposing force of only 2 N. The position-time and error-time graphs of the four performed tests are shown in Figure 9.

The overall performance of the controlled actuator is very good in all four cases. It accurately tracks the ascending parts of the sinusoidal and ramp references, with just a small oscillation around the setpoint of 0.06 and 0.02 mm, respectively. The mean steady-state error during the stationary segments of the ramp, step, and incremental step references varies between 0.01 and 0.03 mm. In the latter two cases, there is no overshoot when reaching the reference and the actuator response is fast, with rise times of 0.84 and 0.31 s, respectively. During the descending parts, the actuator is unable to follow the reference because of the cooling time of the SMA wire and because of the friction between the tendon and the glove and between the tendon and the test bench, which restrains the response of the actuator.

#### Force control

The behavior of the BPID control loop in controlling the output force of the HEMS actuator has also been analyzed.

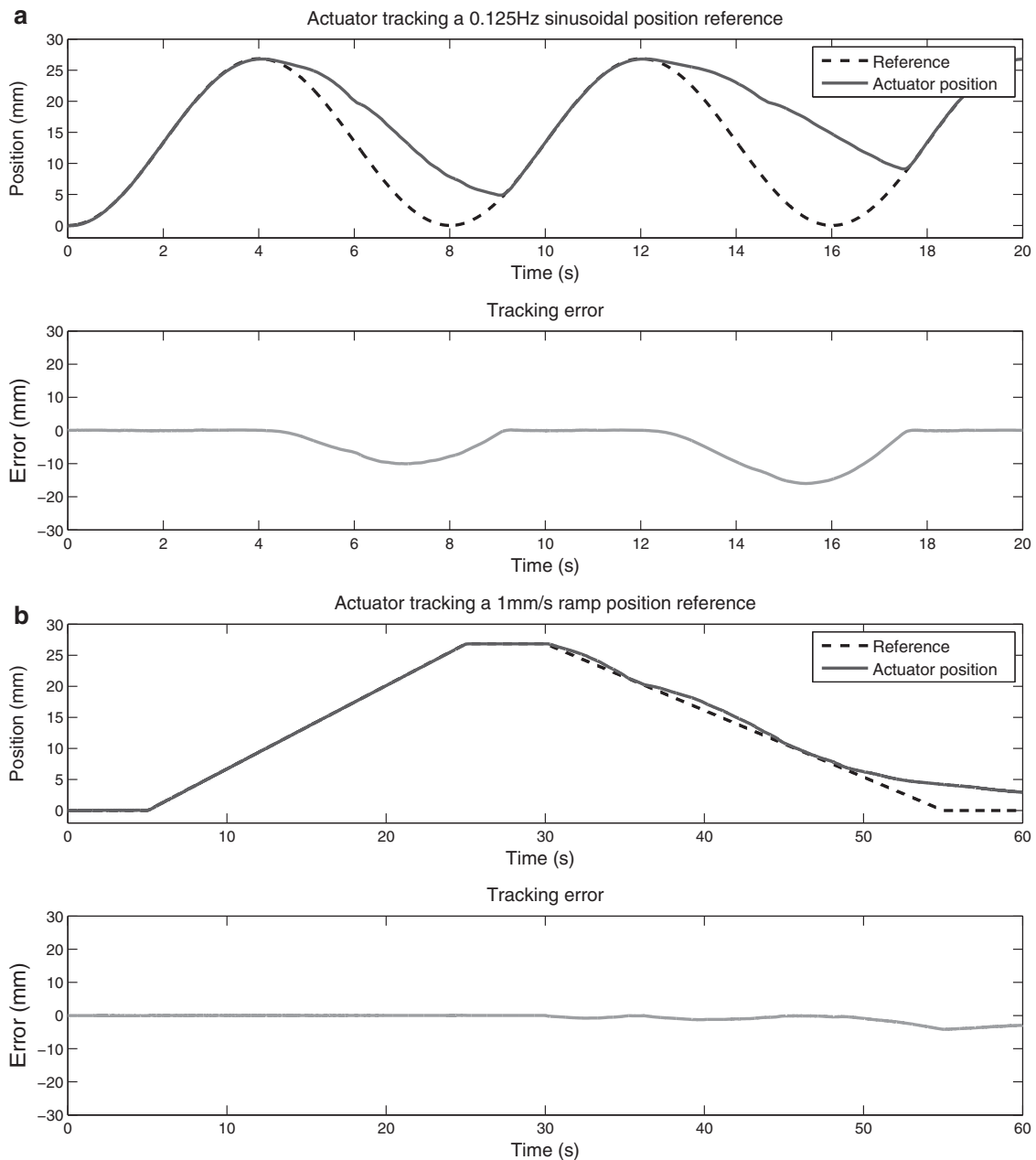


**FIG. 9.** Actuator position and error tracking a: (a) 0.125 Hz sinusoidal reference, (b) ramp reference, (c) step reference, and (d) incremental step reference.

A set of force references similar to those defined for the position control tests has been used. In this case, the maximum amplitude for all references has been 20 N and, after observing that the actuator has a faster response when force controlled than when position controlled, the ramp reference has been replaced by an additional sinusoidal reference at a frequency of 0.25 Hz. The force-time and error-time graphs of the four performed tests are shown in Figure 10.

Considering the response of the actuator shown in the above results, it can be stated that the BPID controller is also suitable to control the force exerted by an SMA actuator. Regarding the accuracy of the controller, even though the noise of the force sensor has a negative impact on its per-

formance, the error is small, with an oscillation around the reference of 0.1 N in the case of the sinusoidal references and a mean steady-state error of 0.05 N for the step reference and 0.04 N for the incremental step references. In these two cases, the rise time is 0.77 and 0.22 s, respectively, and there is no overshoot when reaching the setpoint. During the descending portions of the four references, the response of the actuator is faster than in the position control tests, although it slows down in those parts closest to the initial value.

## Discussion

The results obtained in the characterization tests of the HEMS actuation system suggest that the designed device is

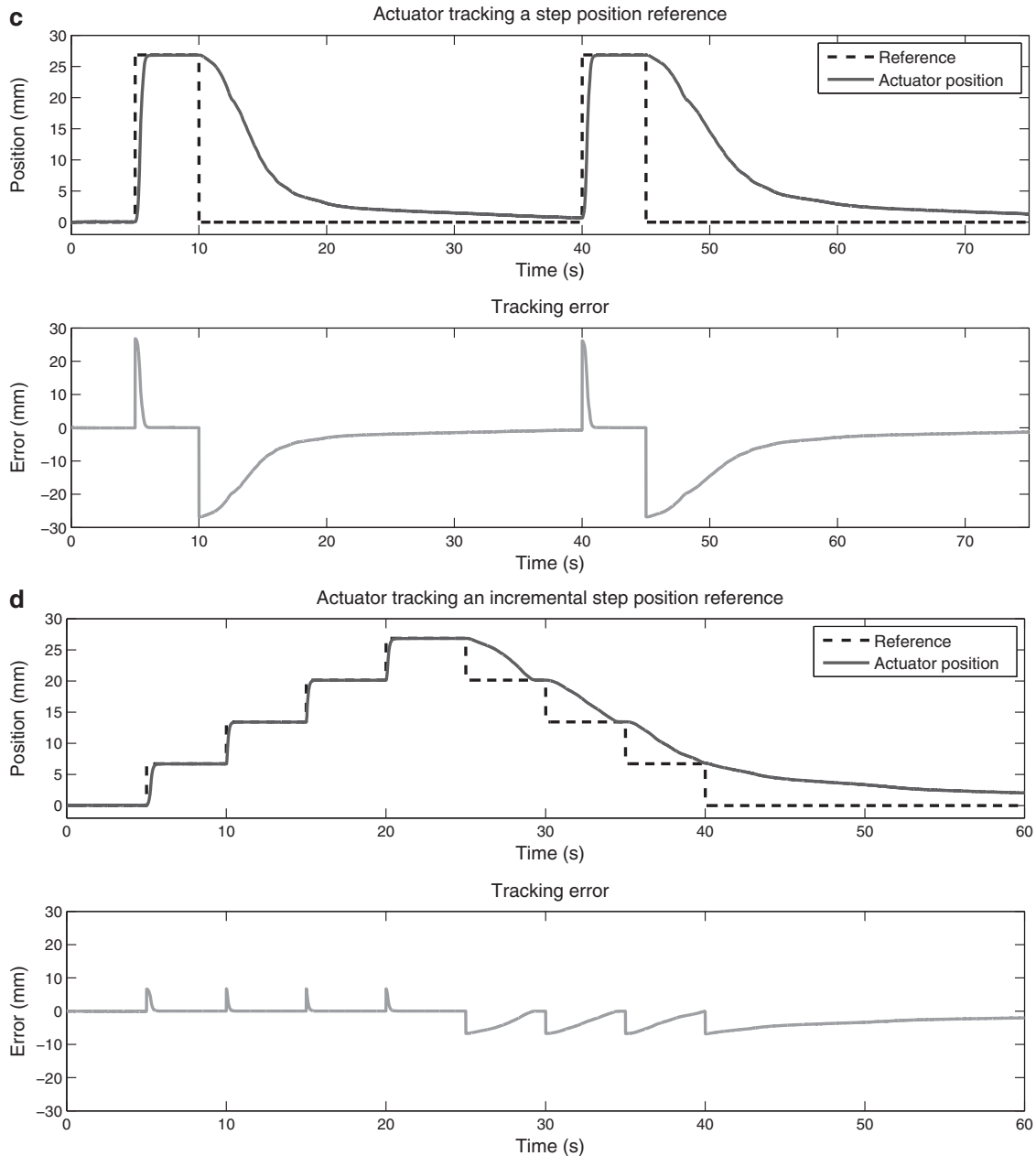


**FIG. 9.** (Continued).

capable of providing at least 50% of the force needed to overcome the opposing forces of a spacesuit glove. Additional experiments should be performed, ideally using a real EVA glove, to assess the extent to which its stiffness is reduced and to experimentally obtain the amount of assistive force provided by the exoskeleton. In addition, for the HEMS to fulfill its intended purpose, a high-level controller should be implemented to allow the user to operate it. For this article, the device has been remotely controlled from a PC, using predefined position and force references. To provide an assistive force proportional to that exerted by the user, the interaction forces between the wearer and the glove should be measured using, for example, fingertip pressure sensors. This information would be processed by the high-level controller

that would generate the necessary commands for the low-level controllers of the actuators so that they exert the required force.

Although the HEMS has been designed according to the soft exoskeleton design paradigm, there are still some rigid and bulky elements that should be redesigned to integrate the device into an EVA spacesuit. For example, the shoulder modules that serve as the attachment point of the fixed end of the actuators have a rather high volume, mainly because of the size of the force sensors they house. This could be easily solved by using a small compression load cell and redesigning the fixed end of the actuators to integrate it. The other element that must be redesigned for the HEMS to better comply with the design principles of soft exoskeletons is the

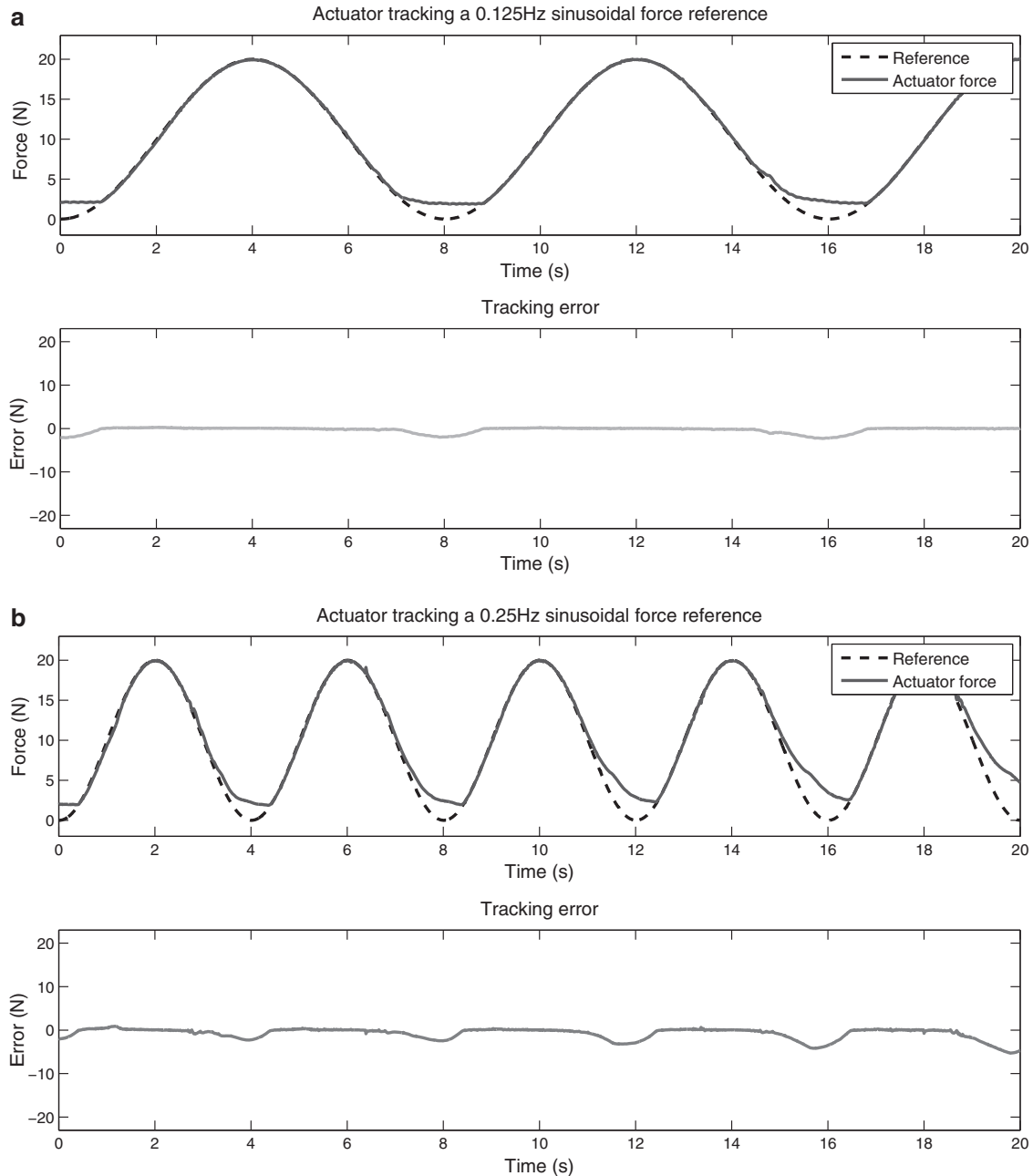


**FIG. 10.** Actuator force and error tracking a: (a) 0.125 Hz sinusoidal reference, (b) 0.25 Hz sinusoidal reference, (c) step reference, and (d) incremental step reference.

sliding platform mechanism that keeps the distance between the base of the fingers and the output of the actuators constant regardless of the position of the hand. Not only is this mechanism rigid, but also adds some complexity to the device and increases the risk of mechanical failure. One possible solution would be to apply the same design concept as in the actuator design, connecting the output of the actuators with the base of the fingers by means of small-diameter flexible sheaths fixed to a compliant piece sewn to the palm of the HEMS internal glove.

The flexible SMA actuator design based on the Bowden transmission system certainly has some features that make it a potential alternative to the use of conventional actuators in

soft exoskeletons, as it solves some of the limiting factors of SMA actuators. The possibility of using long SMA wires inside a flexible body makes it feasible to design an actuator that is able to provide the large displacements often required by soft exoskeletons, and that is easy to integrate and adapt into their flexible and dynamic structures. In addition, the 30% increase of the wire cooling time accomplished, thanks to the multilayer Bowden sheath, results in a higher actuation frequency than that of a bare SMA wire. However, this solution is not exempt of problems. Despite the improvement in the actuation frequency, the actuator speed is still somewhat reduced for those tasks, where the user must make fast movements with his/her fingers. Also, an effect has been

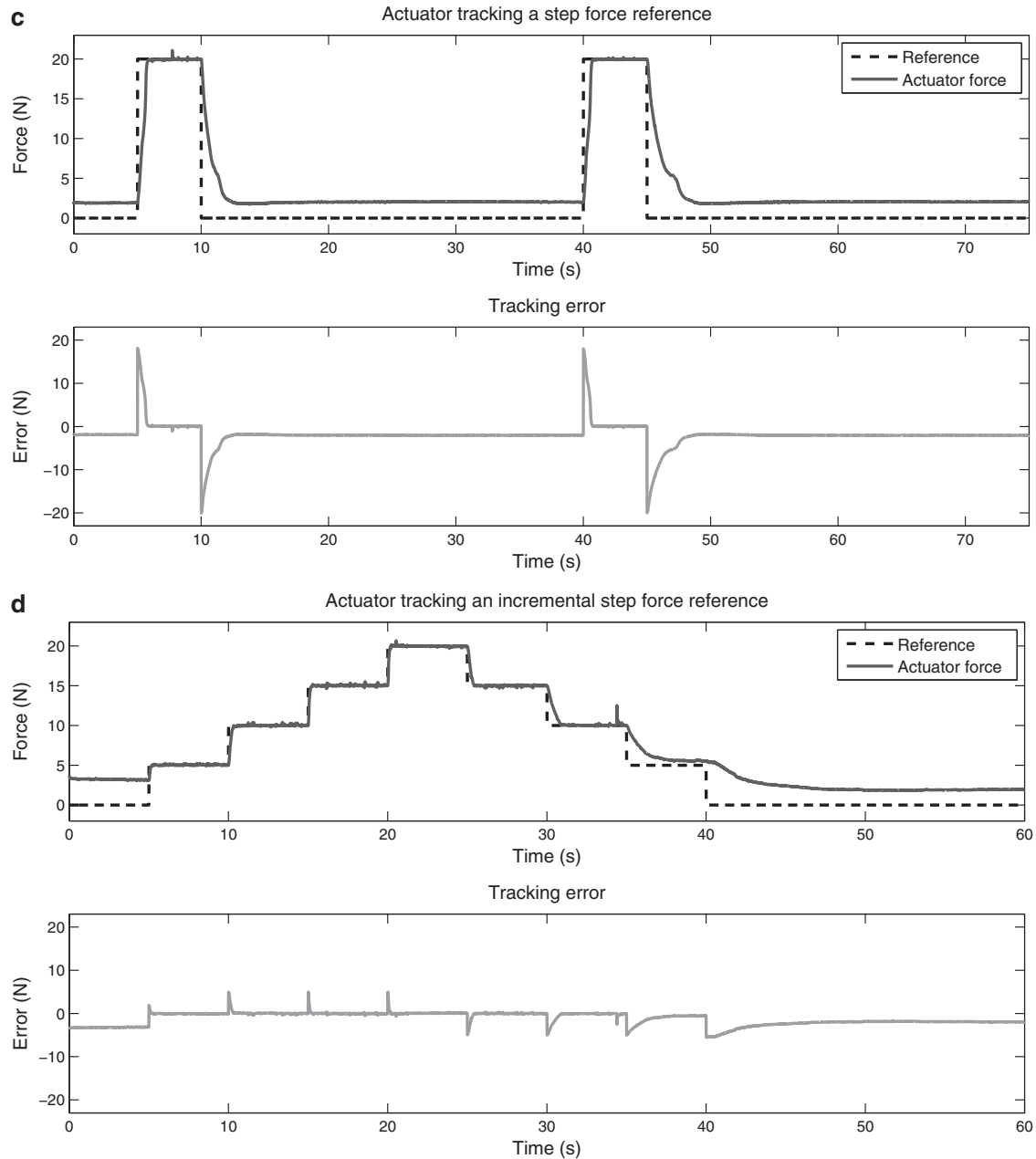


**FIG. 10.** (Continued).

observed which has a negative impact on the operation of the actuator. After several continuous actuation cycles, some of the heat from the SMA wire accumulates in the multilayer sheath, causing the cooling time to slightly increase. This effect can be appreciated in the last actuation cycles of the 0.25 Hz sinusoidal force reference in Figure 10b. A forced convection system that would circulate air around the Bowden sheath to further increase heat rejection could solve this problem.

We believe that this flexible SMA actuator concept has opened a design space that has to be further explored to solve some of the limiting factors of SMA actuators still present in the current design. The cooling time could be greatly improved with a new actuator design consisting of several

thinner wires mechanically arranged in parallel, each of them routed inside an individual small-diameter multilayer Bowden sheath. The combination of the lower cooling time of thinner wires with the improved heat rejection provided by the sheath would significantly increase the actuation bandwidth and, as they would be arranged in parallel, the combined forces of each wire would equal the force of a larger diameter wire.

As a final note, this device, with some modifications, could be used for tasks other than assisting astronauts on EVA missions. For example, its application as a rehabilitation soft exoskeleton is pretty straightforward. The restoring force needed by the SMA actuators to recover their initial length could be provided by a set of antagonistic springs, similarly to

the configuration used in the test bench employed in the experiments. Also, six additional actuators in antagonistic configuration could be used so that the finger extension movement would also be active. In this case, since rehabilitation exercises generally do not require fast movements, the actuation frequency would not be as critical as in the application presented in this article.

## Conclusions

In this article, we have presented the HEMS, a soft hand exoskeleton designed to provide force and motion assistance to astronauts performing EVA by reducing the stiffness of the pressurized spacesuit glove. Designed as a soft exoskeleton because of the advantageous features these devices have for the intended application, the main element of the HEMS is the flexible SMA actuator specifically designed for soft wearable robotic applications. The low profile and flexible design of the actuator allow for an easy integration into the structure of a soft wearable robot, made of textiles and other compliant materials. To be controlled both in position and in force, this actuator includes a position sensor at its moving end and a force sensor at its fixed end.

The flexible body of the designed actuator is a multilayer Bowden sheath, inside which a 90-cm-long SMA wire is routed. The combination of a long SMA wire and a flexible body results in an actuator that generates large output displacements and can adapt its shape to that of the structure where it is installed. In addition, a displacement multiplier mechanism doubles the displacement provided by the SMA wire at the expense of reducing its pulling force by half, resulting in a nominal displacement of 54 mm and a nominal force of 31 N at the actuator output. Thanks to the low friction coefficient of the PTFE inner tube of the multilayer Bowden sheath, frictional losses at the bending points are minimized and the impact on the actuator performance is minimal. Moreover, the helical steel outer sheath increases heat rejection from the SMA wire to its surroundings, as the outer surface of the actuator is greatly increased. This results in a 30% reduction of the cooling time of the SMA wire with respect to a bare wire of the same dimensions and, therefore, a greater actuation frequency.

Regarding the control strategy, the conducted tests show very positive results. After proving in our previous work how the BPID control strategy is a potential alternative for controlling SMA actuators, in this article we have demonstrated that it can also be used to control a device that makes use of such actuators. Moreover, the BPID control strategy has been successfully applied for the first time to implement a force controller for the SMA actuators. The obtained results are very good; the behavior of the actuator is very similar to the one observed when controlled in position, with a high degree of accuracy and stability. Despite the inherent nonlinear behavior of the SMA, the actuator shows no overshoot nor limit cycles in the case of stationary references and the oscillation around the setpoint when following continuously varying references is minimal, in both the position and force control. The only limitation lies on its actuation speed imposed by the cooling time of the SMA wire.

Following the positive results resulting from the evaluation of the HEMS performance, the characterization of the be-

havior of its actuators and the demonstration that the selected control strategy is adequate to control the device both in position and in force, a high-level control system should be implemented so that the device can be used by a human user. For this purpose, a set of fingertip pressure sensors could be used to measure the interaction forces. This information would be used by the force controller to make the SMA actuators reduce or, if possible, eliminate the opposing forces exerted by the internal pressure of an EVA glove. Additional experiments with real subjects should be conducted to assess the range of motion, the comfort of the device, and its ability to perform manipulation tasks.

## Acknowledgments

The research leading to these results has received funding from the STAMAS (Smart Technology for Artificial Muscle Applications in Space) project,\*\* funded by the European Union's Seventh Framework Program for Research (FP7) (Grant No. 312815).

## Author Disclosure Statement

No competing financial interests exist.

## References

1. Strauss S. Extravehicular Mobility Unit Training Suit Symptom Study Report. Technical Report, NASA, 2004.
2. Bishu RR, Klute G. The effects of extra vehicular activity (EVA) gloves on human performance. *Int J Ind Ergon* 1995;16:165–174.
3. Mesloh M, England S, Benson E, *et al.* The effects of extravehicular activity (EVA) glove pressure on hand strength. In: 3rd International Conference on Applied Human Factors and Ergonomics, San Francisco, CA: AHFE, 2010.
4. Appendino S, Battezzato A, Chen FC, *et al.* Effects of EVA spacesuit glove on grasping and pinching tasks. *Acta Astronautica* 2014;96:151–158.
5. Appendino S, Ambrosio EP, Chen FC, *et al.* Effects of EVA glove on hand performance. In: 41st International Conference on Environmental Systems, Portland, OR: AIAA, 2011.
6. Mousavi M, Appendino S, Battezzato A, *et al.* Stiffness of an EVA glove: objective evaluation and testing procedures. In: 12th Symposium on Advanced Space Technologies in Robotics and Automation (ASTRA), Noordwijk, The Netherlands: Copernicus Publications, 2013.
7. Walz C, Gernhardt M. Extravehicular activity—challenges in planetary exploration. In: 3rd Space Exploration Conference and Exhibit, Denver, CO: AIAA and NASA, 2008.
8. Main JA, Peterson SW, Strauss AM. A prototype power assist EVA glove. In: 21st International Conference on Environmental Systems, San Francisco, CA: SAE International, 1991.
9. Main JA, Peterson SW, Strauss AM. Power assist EVA glove development. In: 22nd International Conference on Environmental Systems, Seattle, WA: SAE International, 1992.
10. Sorenson EA, Sanner RM, Howard RD, *et al.* Development of a power-assisted space suit glove joint. In: 27th International Conference on Environmental Systems, Lake Tahoe, NV: SAE International, 1997.

---

\*\*www.stamas.eu



11. Sorenson E, Sanner R, Ranniger C. Experimental testing of a power-assisted space suit glove joint. *Comput Cybern Simul* 1997;3:2619–2625.
12. Yamada Y, Morizono T, Sato S, *et al.* Proposal of a Skil-Mate finger for EVA gloves. In: 2001 IEEE International Conference on Robotics and Automation (ICRA), volume 2, Seoul, South Korea: IEEE, 2001, pp. 1406–1412.
13. Pillsbury TE, Kothera CS, Wereley NM, *et al.* Pneumatically power assisted extra-vehicular activity glove. In: 45th International Conference on Environmental Systems, Bellevue, WA: AIAA, 2015.
14. Favetto A, Chen FC, Ambrosio EP, *et al.* Towards a hand exoskeleton for a smart EVA glove. In: 2010 IEEE International Conference on Robotics and Biomimetics (ROBIO), Tianjin, China: IEEE, 2010, pp. 1293–1298.
15. Favetto A, Ambrosio EP, Appendino S, *et al.* A preliminary study towards an EVA glove exoskeleton. In: 11th Symposium on Advanced Space Technologies in Robotics and Automation (ASTRA), Noordwijk, The Netherlands: Copernicus Publications, 2011.
16. Favetto A, Ambrosio EP, Appendino S, *et al.* Embedding an exoskeleton hand in the astronaut's EVA glove: feasibility and ideas. *Int J Aerospace Sci* 2012;1:68–76.
17. Shields B, Main J, Peterson S, *et al.* An anthropomorphic hand exoskeleton to prevent astronaut hand fatigue during extravehicular activities. *IEEE Trans Syst Man Cybern Syst Hum* 1997;27:668–673.
18. Favetto A. *Glove Exoskeleton for Extra-Vehicular Activities—Analysis of Requirements and Prototype Design*, PhD Thesis, Politecnico di Torino, 2014.
19. Matheson E, Brooker G. Augmented robotic device for EVA hand manoeuvres. *Acta Astronautica* 2012;81:51–61.
20. Rocon E, Ruiz AF, Raya R, *et al.* Human-robot physical interaction. In: Pons JL, ed. *Wearable Robots: Biomechatronic Exoskeletons*. Chichester, UK: John Wiley & Sons; 2008;127–163.
21. Nilsson M, Ingvast J, Wikander J, *et al.* The soft extra muscle system for improving the grasping capability in neurological rehabilitation. In: 2012 IEEE-EMBS Conference on Biomedical Engineering and Sciences, Langkawi, Malaysia: IEEE, 2012, pp. 412–417.
22. Fausti D, Seneci C. *Hand Rehabilitation Device*, United States, US 2013/0072829 A1, 2013.
23. Delph MA, Fischer SA, Gauthier PW, *et al.* A soft robotic exomusculature glove with integrated sEMG sensing for hand rehabilitation. *IEEE Int Conf Rehabil Robot* 2013; 2013:6650426.
24. Nycz CJ, Delph MA, Fischer GS. Modeling and design of a tendon actuated soft robotic exoskeleton for hemiparetic upper limb rehabilitation. In: 2015 37th Annual International Conference of the IEEE Engineering in Medicine and Biology Society (EMBC), Milan, Italy: IEEE, 2015, pp. 3889–3892.
25. In H, Kang BB, Sin M, *et al.* Exo-Glove: a wearable robot for the hand with a soft tendon routing system. *IEEE Robot Autom Mag* 2015;22:97–105.
26. Polygerinos P, Wang Z, Galloway KC, *et al.* Soft robotic glove for combined assistance and at-home rehabilitation. *Rob Auton Syst* 2015;73:135–143.
27. Polygerinos P, Galloway KC, Savage E, *et al.* Soft robotic glove for hand rehabilitation and task specific training. In: 2015 IEEE International Conference on Robotics and Automation (ICRA), Seattle, WA: IEEE, 2015, pp. 2913–2919.
28. Polygerinos P, Galloway KC, Sanan S, *et al.* EMG controlled soft robotic glove for assistance during activities of daily living. In: 2015 IEEE International Conference on Rehabilitation Robotics (ICORR), Singapore: IEEE, 2015, pp. 55–60.
29. Yap HK, Lim JH, Nasrallah F, *et al.* A soft exoskeleton for hand assistive and rehabilitation application using pneumatic actuators with variable stiffness. In: 2015 IEEE International Conference on Robotics and Automation (ICRA), Seattle, WA: IEEE, 2015, pp. 4967–4972.
30. Thompson-Bean E, Steiner O, McDaid A. A soft robotic exoskeleton utilizing granular jamming. In: 2015 IEEE International Conference on Advanced Intelligent Mechatronics (AIM), Busan, Korea: IEEE, 2015, pp. 165–170.
31. Galloway KC, Polygerinos P, Walsh CJ, *et al.* Mechanically programmable bend radius for fiber-reinforced soft actuators. In: 2013 16th International Conference on Advanced Robotics (ICAR), Montevideo, Uruguay: IEEE, 2013, pp. 1–6.
32. Maeder-York P, Clites T, Boggs E, *et al.* Biologically inspired soft robot for thumb rehabilitation. *J Med Dev* 2014; 8:(020933)1–(020933)3.
33. Freni P, Botta EM, Randazzo L, *et al.* Innovative hand exoskeleton design for extravehicular activities in space. In: Pernici B, Della Torre S, Colosimo BM, Faravelli T, Paolucci R, Piardi S, eds. *SpringerBriefs in Applied Sciences and Technology* Milan, Italy: Springer International Publishing, 2014.
34. Diftler MA, Ihrke CA, Bridgwater LB, *et al.* RoboGlove—a grasp assist device for earth and space. In: 45th International Conference on Environmental Systems, Bellevue, WA: AIAA, 2015.
35. Rogers JM, Peters BJ, Laske EA, *et al.* Initial work toward a robotically assisted extravehicular activity glove. In: 46th International Conference on Environmental Systems, Vienna, Austria: AIAA, 2016.
36. Rogers JM, Peters BJ, Laske EA, *et al.* Development and testing of robotically assisted extravehicular activity gloves. In: 47th International Conference on Environmental Systems, Charleston, SC: AIAA, 2017.
37. Sutter PH, Iatridis JC, Thakor NV. Response to reflected-force feedback to fingers in teleoperations. In: *NASA Conference on Space Telerobotics*, volume 4, Pasadena, CA: NASA, 1989, pp. 65–74.
38. Hadi A, Alipour K, Kazeminasab S, *et al.* Design and prototyping of a wearable assistive tool for hand rehabilitation using shape memory alloys. *ASME 2016 Conference on Smart Materials, Adaptive Structures and Intelligent Systems*. American Society of Mechanical Engineers, 2016:1–7.
39. Hirose S, Ikuta K, Umetani Y. Development of shape-memory alloy actuators. Performance assessment and introduction of a new composing approach. *Adv Robot* 1988; 3:3–16.
40. Dittmer DK, Buchal RO, MacArthur DE, *et al.* The SMART wrist-hand orthosis (WHO) for quadriplegic patients. *J Prosthet Orthot* 1993;5:73.
41. Tang T, Zhang D, Xie T, *et al.* An exoskeleton system for hand rehabilitation driven by shape memory alloy. 2013 IEEE International Conference on Robotics and Biomimetics (ROBIO). IEEE, 2013:756–761.
42. Hamid AMB, Makhdoomi MR, Saleh T, *et al.* Development of a shape memory alloy (SMA) based assistive hand. *Adv Mater Res* 2015;1115:454–457.

43. Villoslada A, Flores A, Copaci D, *et al.* High-displacement fast-cooling flexible shape memory alloy actuator: application to an anthropomorphic robotic hand. In: 2014 14th IEEE-RAS International Conference on Humanoid Robots, Madrid, Spain: IEEE, 2014, pp. 27–32.
44. Villoslada A, Flores A, Copaci D, *et al.* High-displacement flexible shape memory alloy actuator for soft wearable robots. *Rob Auton Syst* 2015;73:91–101.
45. Villoslada A, Escudero N, Martín F, *et al.* Position control of a shape memory alloy actuator using a four-term bilinear PID controller. *Sens Actuators A Phys* 2015;236: 257–272.
46. Butera F, Biasiotto M, Alacqua S. Actuator Device with a Flexible Cable Incorporating a Shape-Memory Element, United States, US 6732516 B2, 2004.
47. Neugebauer R, Pagel K, Bucht A, *et al.* Model-based position control of shape memory alloy actuators. *Int J Mechatron Manuf Syst* 2012;5:93–105.
48. DYNALLOY, Inc. Technical Characteristics of Flexinol Actuator Wires. Irvine, CA: DYNALLOY, Inc., 2014.
49. Ma N, Song G. Control of shape memory alloy actuator using pulse width modulation. *Smart Mater Struct* 2003;12:712–719.
50. Martineau S, Burnham KJ, Haas OCL, *et al.* Four-term bilinear PID controller applied to an industrial furnace. *Control Eng Pract* 2004;12:457–464.
51. Schiele A, Letier P, van der Linde R, *et al.* Bowden cable actuator for force-feedback exoskeletons. In: 2006 IEEE/RSJ International Conference on Intelligent Robots and Systems, Beijing, China: IEEE, 2006, pp. 3599–3604.

Address correspondence to:

Álvaro Villoslada

Carlos III University

Av. de la universidad, 30

Lab. 1.3.C13

Leganés, 28911

Madrid

Spain

E-mail: alvaro.villoslada@uc3m.es